# Direct Loading of the Purified Endogenous Inhibitor into the Cytoplasm of Patched Cardiomyocytes Blocks the Ion Currents and Calcium Transport through the NCX1 Protein[†]

Liron Boyman,[‡] Reuben Hiller,[‡] W. Jonathan Lederer,[§] and Daniel Khananshvili*[,‡]

*Department of Physiology and Pharmacology, Sackler School of Medicine, Tel-Aviv University, Ramat-Aviv 69978, Israel, and Medical Biotechnology Center, University of Maryland Biotechnology Institute, Baltimore, Maryland 21201*

*Received March 16, 2008; Revised Manuscript Received April 30, 2008*

ABSTRACT: The $Na^+-Ca^{2+}$ exchanger in mammalian heart muscle (NCX1) is the central transporter protein that regulates extrusion of $Ca^{2+}$ from the heart cell. However, the functional biochemistry and physiology of NCX1 have been severely hampered by the absence of any specific high-affinity inhibitor. Here we describe advanced procedures for purifying a candidate inhibitor, previously called endogenous inhibitor factor ($NCX_{IF}$), and demonstrate its direct actions on NCX1 activities in the single-cell system. A combination of advanced HILIC (hydrophilic interaction liquid chromatography) procedures with analytical tests suggests that the properties of $NCX_{IF}$ resemble those of a small (disaccharide size) polar molecule lacking any aromatic rings, conjugated bonds, or a primary amino group. The effects of $NCX_{IF}$ on the NCX1-mediated ion currents ($I_{NCX}$) and cytosolic $Ca^{2+}$ extrusion were detected by a combination of patch-clamp and confocal microscopy under conditions in which the purified $NCX_{IF}$ was directly loaded into the cytoplasm of patched cardiomyocytes. It was demonstrated that cytosolic $NCX_{IF}$ blocks the $Ca^{2+}$-activated NCX1 inward current and the accompanying extrusion of $Ca^{2+}$ from the cell with high efficacy. A constant fraction of NCX1 inhibition was observed under conditions in which the cytosolic $[Ca^{2+}]_i$ was varied at fixed doses of $NCX_{IF}$, suggesting that the degree of inhibition is controlled by $NCX_{IF}$ dose and not by cytosolic $Ca^{2+}$ concentration. $NCX_{IF}$ blocks equally well both the $Ca^{2+}$ extrusion and $Ca^{2+}$ entry modes of NCX1, consistent with thermodynamic principles expected for the functioning of a bidirectional "carrier-type" transport system. We concluded that $NCX_{IF}$ interacts with a putative regulatory domain from the cytosolic side and, thus, may play an important regulatory role in controlling $Ca^{2+}$ signaling in the heart. This may represent a new potential tool for developing novel treatments for cardiac $Ca^{2+}$ signaling dysfunction.

Proteins of the NCX gene family contribute to $Ca^{2+}$ regulation in many cell types (*1–4*), with three genes responsible for expression, namely, NCX1, NCX2, and NCX3, with multiple splice variants (*2, 5–7*). In heart, the electrogenic $Na^+-Ca^{2+}$ exchange (*8*) is due to the gene product of NCX1.1, and although the molecular and biophysical properties have been broadly studied (*2–7*), endogenous regulation is incompletely understood (*9–13*). Nevertheless, it is clear that changes in NCX1 protein expression accompany the development of diverse diseases such as heart failure and arrhythmia (*2–4, 9*). There is, however, considerable uncertainty regarding the role played by NCX1 in these diseases; moreover, to date, there is no evidence that the NCX1 activity is the primary cause of such diseases, nor are mutations of NCX1 linked to any specific disease. Nevertheless, NCX1 protein levels may change and certainly contribute to $Ca^{2+}$ transport and signaling dysfunction, although the details remain poorly understood (*2–4, 9*).

The $Na^+-Ca^{2+}$ exchange turnover rate is clearly affected by the intracellular $Ca^{2+}$, $Na^+$, and $H^+$ ions, which interact with the regulatory cytosolic f-loop of NCX proteins (*3, 4, 10–13*). Other cellular factors (ATP, $PIP_2$, and lipids) also can modulate NCX1, but their physiological relevance is still unclear (*11, 12*). No phosphorylation of the cardiac NCX1 protein has been demonstrated either in vitro or in vivo. Recent breakthroughs in elucidating the three-dimensional structure revealed that the f-loop contains two $Ca^{2+}$-binding domains, CBD1 and CBD2 (*14–16*), which may modulate the NCX1 activity by sensing the cytosolic $Ca^{2+}$ concentrations. If specific endogenous factors exist, affecting the $Ca^{2+}$ interactions with the cytosolic regulatory domains, they may be quite important.

We isolated (from calf ventricle extracts) and purified a low-molecular mass substance that inhibits NCX1 in sarcolemma vesicles (*17, 18*). Mass spectroscopic and gel filtration analyses of active fractions revealed a small (350−550 Da)

[†] This work was funded by the USA-Israeli Binational Foundation, Research Grant 2003-372 (D.K. and W.J.L.), the Israeli Ministry of Health, Research Grant 3000003019 (D.K.), the National Heart, Lung and Blood Institute, and MBC-UMBI initiative funds (W.J.L.). The Ph.D. stipend of L.B. was supported by the Dr. Miriam and Sheldon G. Edelson Foundation.

* To whom correspondence should be addressed: Department of Physiology and Pharmacology, Sackler School of Medicine, Tel-Aviv University, Ramat-Aviv 69978, Israel. Telephone: 972-3-640-9961. Fax: 972-3-640-9113. E-mail:dhanan@post.tau.ac.il.

[‡] Tel-Aviv University.

[§] University of Maryland Biotechnology Institute.

10.1021/bi8004279 CCC: $40.75 © 2008 American Chemical Society
Published on Web 05/29/2008

polar molecule that is not retained on the regular RP-HPLC columns (*17, 18*). Chemical tests and spectroscopic analyses showed no content for conjugated bonds, aromatic rings, primary amines, or aldehyde groups, the properties thereby resembling those of nonreducing "sugarlike" molecules (*17, 18*). This low-abundance compound inhibits NCX1 activities in the range of $10^{-6}-10^{-7}$ M (*18*), but it has no effect on the $Na^+/K^+$-ATPase or SR $Ca^{2+}$-ATPase activities (*19*). This compound was termed "the NCX inhibitory factor" ($NCX_{IF}$).

Application of $NCX_{IF}$ to organ bath solutions elevates the contractility of ventricle strips (*17, 20*), meaning that $NCX_{IF}$ could be a physiologically active substance. Importantly, the $\beta_1$-blocker (deraline) does not affect these actions (*20*), suggesting that $NCX_{IF}$ may act through a mechanism that is independent of the $\beta$-adrenergic pathway. Moreover, $NCX_{IF}$ could suppress ouabain-induced arrhythmias, the properties thereby resembling those of antiarrhythmic agents (*23*). This suppression of arrhythmia may represent the $NCX_{IF}$-induced block of $Ca^{2+}$-activated inward $I_{NCX}$ (triggered during $Ca^{2+}$ overload).

Extracellular perfusion of electrically paced cardiomyocytes with $NCX_{IF}$ resulted in enhanced amplitudes of cell contractions and of $[Ca^{2+}]_i$ transients (*22*). Although these observations can be rationally explained by primary inhibition of NCX1 in the cell, no evidence existed for this claim. The reason for this lack of information was that no patch-clamp techniques were applied at this time for testing the $NCX_{IF}$ effects in a single-cell system. Therefore, in this work the effects of $NCX_{IF}$ on $I_{NCX}$ currents and $Ca^{2+}$ extrusion were tested under conditions in which $NCX_{IF}$ was directly loaded into the cytoplasm of patched cardiomyocytes. Here, the cytosolic $[Ca^{2+}]_i$ was transiently elevated (by exposing cardionyocytes to caffeine for short periods), whereas the $I_{NCX}$ and $[Ca^{2+}]_i$ signals were subsequently recorded with patch-clamp and confocal microscopy.

If NCX1 is affected by $NCX_{IF}$, it is also important to know where on the protein $NCX_{IF}$ acts. Kinetic studies with sarcolemma vesicles suggested that $NCX_{IF}$ acts as a noncompetitive inhibitor with respect to extravesicular (cytosolic) $Ca^{2+}$ (*21*). This was taken to mean that $NCX_{IF}$ interacts with a regulatory (but not transport) site on NCX1 protein and may thereby alter the rate-limiting step of the ion transport cycle. In intact cells, the time of action of extracellularly applied $NCX_{IF}$ on contractility and $[Ca^{2+}]_i$ transients was quite slow (5−15 min), suggesting that $NCX_{IF}$ must enter the cell to act (*20, 22*). To test the sidedness of the action of $NCX_{IF}$, we directly loaded purified $NCX_{IF}$ into the cytoplasm through the patch-clamp electrode and examined the action of $NCX_{IF}$ on $I_{NCX}$ and $Ca^{2+}$ extrusion. We provide strong evidence that $NCX_{IF}$ blocks NCX1 from the inside of the cell with great efficacy, meaning that $NCX_{IF}$ may be an endogenous regulator of $Ca^{2+}$ transport through the regulation of NCX1 in intact cells.

## MATERIALS AND METHODS

*Materials and Reagents.* Protease inhibitors (PMSF, pepstatin, leupeptin, and aprotenin), deoxyribonuclease I (type DN-25), fluorescamine,[1] Dowex-50W 1X8, Dowex-AG 1X4, and laminin were obtained from Sigma (St. Louis, MO). Sephadex G-10 (fine) was from Pharmacia (Uppsala, Sweden). The glass microfiber filters (GF/C Whatman) were purchased from Tamar (Jerusalem, Israel). Chelex 100 was obtained from Bio-Rad. $^{45}CaCl_2$ (10−30 mCi/mg) was purchased from DuPont NEN (Boston, MA) or Perkin-Elmer (Monza, Italy). Fluo-4 ($K_5$) and Fluo-3 AM were from Teflabs (Austin, TX), Biotium (Toronto, ON), or Molecular Probes (Eugene, OR). The following reagents were used for preparing cardiomyocytes: penicillin streptomycin (Biological Industries, Haemek, Israel), bovine calf serum (Hyclone), collagenase II (Worthington), and trypsin, minimal essential medium-1, and L-glutamine (Gibco Invitrogen). The scintillation cocktail Opti-Fluor was from Packard (Groningen, The Netherlands). All other reagents were analytical or HPLC grade. Deionized water (18 MΩ/cm, Millipore system) was used for preparing solutions.

*Effect of $NCX_{IF}$ on $Na_i$-Dependent $^{45}Ca$ Uptake in Sarcolemma Vesicles.* The sarcolemma vesicles were obtained according to established procedures (*27, 28*). The $Na_i$-dependent $^{45}Ca$ uptake was initiated by rapid dilution of Na-loaded vesicles in an assay medium containing $^{45}Ca$ with lipid/protein-free aliquots of $NCX_{IF}$ (*17–21*). The inhibitory capacity of $NCX_{IF}$ preparations was quantitatively evaluated in arbitrary inhibitory units (one inhibitory unit represents the amount of $NCX_{IF}$ that inhibits the $Na_i$-dependent $^{45}Ca$ uptake by 1% under fixed experimental conditions) (*17–23*). The samples can be stored at −70 °C without any loss of inhibitory activity of $NCX_{IF}$ for at least 8−12 months.

*Extraction and Precolumn Purification of $NCX_{IF}$.* $NCX_{IF}$ was extracted from 6−8 kg of calf ventricle muscle with 95% ethanol, as previously described (*17–23*). Briefly, after ethanol was evaporated, the remaining aqueous phase was reduced to 0.3−0.5 L and insoluble material was removed by centrifugation (20000*g* for 30 min). From the supernatant, lipids were removed with chloroform, and cold ethanol (−20 °C) was added to the aqueous phase (to yield ∼80%). White precipitate was removed by centrifugation, and after ethanol was evaporated, cold acetone was added to yield ∼90%. White precipitate was removed by centrifugation, and concentrated material (100−150 mL) was passed through equal volumes of Dowex 2X8 (acetate form) and Dowex 50W ($H^+$ form) slurry. The collected effluents were reduced to 50−80 mL (yellow-brown color) and then passed through the CarbPacking SPE (60 mL/10 g) cartridge (Supelco, Bellefonte, PA). The nearly colorless effluent (30−50 mL) was loaded onto the Sephadex G-10 column (5.5 cm × 70 cm) and flushed with water (2 mL/min). The fractions containing the $NCX_{IF}$ activity were concentrated, filtered, and stored at −70 °C until they were purified further (*17, 18*).

[1] Abbreviations: Arsenazo III, 2,2′-(1,8-dihydroxy-3,6-disulfonaphthylene-2,7-bisazo)bisbenzenearsonic acid; Fluo-3, *N*-(2-{2-[bis(carboxymethyl)amino]-5-(2,7-dichloro-6-hydroxy-3-oxy-3*H*-xanthen-9-yl)henoxy]ethoxy}-4-methylphenyl)-*N*-(carboxymethyl)glycine; fluorescamine, 4-phenylspiro[furan-2(3*H*),1′-phthalan]-3,3-dione; FRCRCFa, S−S bond cyclic hexapeptide Phe-Arg-Cys-Arg-Cys-Phe-$NH_2$; XIP, inhibitory peptide containing 20 amino acids; LC−MS, liquid chromatography coupled with mass spectroscopy; LC−MS/MS, liquid chromatography coupled with MS/MS; Mops, 3-(*N*-morpholino)propanesulfonic acid; Tris, tris(hydroxymethyl)aminomethane; PMSF, phenylmethanesulfonyl fluoride; TMA, tetramethylammonium.

*Chromatography.* Fully computerized HPLC systems were used for $NCX_{IF}$ purification, as described in previous publications (*18–23*). A combination of RP-HPLC and HILIC HPLC columns was used in this work for $NCX_{IF}$ purification: Synergi Polar (Phenomenex; 250 mm × 21 mm, 4 μm), TSK-gel Amide-80 (TosoHaas, Ltd.; 21 mm × 300 mm, 7 μm), Krumasil Silica 100A (Phenomenex; 250 mm × 21.2 mm, 5 μm), apHera-$NH_2$ (Astec; 250 mm × 4.6 mm, 5 μm), Cyclobond I 2000, β-cyclodextran (Astec; 250 mm × 4.6 mm, 5 μm), ZIC-*p*HILIC (SeQuant; 150 mm × 4.6 mm, 5 μm), and Aminex HPX-87c (Bio-Rad 250 mm × 4 mm, 9 μm). For HILIC columns, the injecting samples were dissolved in 80−95% methanol. All HPLC columns were run at 22−25 °C, besides the Aminex column, which was explored at 60−80 °C.

*Preparation of Cardiomyocytes.* Isolated ventricular myocytes were obtained from adult female Sprague-Dawley rats (225−250 g). Briefly, rats were deeply anesthetized with sodium pentobarbital (0.1 mg/g ip) and heparinized (1.25 units/g ip). Fifteen minutes after heparin was injected, the heart was rapidly excised and rinsed with cold 250 μM EGTA isolation buffer containing 130 mM NaCl, 1 mM lactic acid, 5.4 mM KCl, 3 mM sodium pyruvate, 25 mM HEPES, 0.5 mM $MgCl_2$, 0.33 mM $NaH_2PO_4$, 22 mM D-glucose, and 0.01 unit/mL insulin (pH 7.4) (adjusted with NaOH). The aorta was quickly cannulated for Langendorff perfusion. The heart coronary arteries were perfused at 37 °C for 2 min with EGTA isolation buffer and then perfused for 8 min with the same buffer supplemented with 50 μM $CaCl_2$, 1.6 mg/mL collagenase (type II; Worthington Biochemical, Lakewood, NJ), and 0.04 mg/mL protease (XIV). The ventricles were cut down, minced, and then gently agitated for 4 min in isolation buffer containing 83 μM $CaCl_2$, 1 mg/mL collagenase, 0.066 mg/mL protease, and 1.66% BSA. The cells were filtered through nylon mesh (300 μm) and, after being washed, were resuspended, in succession, in enzyme-free isolation buffer (1% BSA) containing 250 and 500 μM $CaCl_2$. After a final wash, the cardiomyocytes were resuspended at room temperature in the cell medium (17.4 mg/mL HEPES-buffered DMEM) supplemented with 10% fetal calf serum (Gibco), 0.01 unit/mL insulin, and 44 mM NaCl (pH 7.4) (adjusted with NaOH).

*Simultaneous Measurements of $I_{NCX}$ and $[Ca]_i$ by Patch-Clamp and Confocal Microscopy.* A patch-clamp method was combined with confocal $Ca^{2+}$ imaging microscopy to enable simultaneous measurement of $I_{NCX}$ and $[Ca]_i$ recordings in single cardiomyocytes exposed to a submaximal but high level (5 mM) of caffeine (*24–26*). To this end, freshly isolated cardiomyocytes were attached to laminin-coated coverslips and used within 4−5 h. Only quiescent, rod-shaped myocytes with clear striations were used. Experiments were performed at room temperature (20−23 °C). The Giga-Ohm seal was attained while superfusing the recording chamber with normal Tyrode containing 140 mM NaCl, 10 mM D-glucose, 2 mM $CaCl_2$, 10 mM HEPES, 1 mM $MgCl_2$, and 4 mM KCl (pH 7.4) (adjusted with NaOH). The patch pipet (1.8−2.2 MΩ) was filled with a solution that contained 2.5 mM $Na_2ATP$, 2.5 mM MgATP, 2.5 mM $MgCl_2$, 30 mM KCl, 110 mM potassium aspartic acid, 10 mM HEPES, 0.05 mM Fluo-4 ($K_5$) (Molecular Probes) (pH 7.2) (adjusted with KOH). After the whole-cell patch clamp was established, the cells were superfused with normal Tyrode supplemented with 5 mM 4-aminopyridine and 0.1 mM $BaCl_2$. Cells were loaded for 8−10 min with Fluo-4 through the patch pipet before the experiments were started. Voltage control and recordings were performed with an Axopatch 200A amplifier and Digidata 1322A (Axon Instruments). Currents were low-pass filtered at 1 kHz and sampled at 2 kHz. All currents were normalized to cell capacitance to account for differences in cell size, and data are reported as current densities (picoamperes per picofarad). Cell capacitance was calculated from the capacity transient elicited by 10 ms hyperpolarization pulses from −90 to −95 mV. To elicit $I_{NCX}$, the patched cardiomyocyte was held at −80 mV, and 5 mM caffeine was locally applied for 5 s by a Pneumatic Pico Pump (PV830, World Precision Instruments, Inc.). $[Ca]_i$ imaging was performed with a Zeiss (LSM510) laser scanning confocal microscope equipped with an argon laser and a 63× 1.4 NA oil immersion objective (Zeiss). The scanned line was positioned along the longitudinal axis of the cardiomyocyte; Fluo-4 was excited at 488 nm, and the fluorescence above 505 nm was recorded. Line-scan images (time vs *x*) were acquired at a sampling rate of 1.92 ms/line. Caffeine application was repeated every 7 min for as long as the cardiomyocytes remained quiescent; the leak currents were stable and <200 pA. To keep the cardiomyocytes undamaged due to the caffeine exposure, 5 mM caffeine was used in all experiments.

*Detection of the $Ca^{2+}$ Entry and $Ca^{2+}$ Exit Modes of NCX1 in Single Cardiomyocytes.* The forward and reverse modes of NCX1 were measured in Fluo-3-loaded rat cardiomyocytes, according to established protocols (*33, 34*). In these experiments, the SR function was completely blocked by pretreatment of cardiomyocytes with 10 μM ryanodine and 1 μM thapsigargin. To assess the $Ca^{2+}$ entry via NCX1, we abruptly replaced the extracellular NaCl (137 mM) with the same concentration of TMA for 20 s. The $Ca^{2+}$ exit mode was induced by replacing 137 mM TMA with 137 mM NaCl. The $[Ca^{2+}]_i$ in cardiomyocytes was detected with Fluo-3 by using wide-field fluorescence microscopy (*22*). The prepared coverslips, containing Fluo-3-loaded cardiomyocytes, were placed in a recording chamber on the stage of an inverted microscope (Olympus IX-71). The chamber was perfused with the following: 137 mM NaCl, 4 mM KCl, 1.2 mM $MgSO_4$, 10 mM glucose, 10 mM HEPES, and 1.5 mM $CaCl_2$ (pH 7.4) at 27 °C with a temperature controller system (Automatic Temperature Controller, TC-324B, Warner). The excitation light (mercury burner, 100 W, Osram) was passed through a set of neutral density and excitation filters (HQ480, Chroma) and focused with a 40× objective (LCPlanF1, Olympus) and field diaphragm (allowing full illumination of single cardiomyocytes). Next, the emitted fluorescence was filtered through the dichroic mirror (Q505LP, Chroma) and emission filter (HQ535, Chroma). The fluorescence signal was recorded with a photon counting device (C&L Instruments) and digitized with a PCI-DAQ card. Each experiment was recorded and stored as a separate file by using Chart version 4.12 (ADInstruments). After subtraction of autofluorescence, the Fluo-3-recorded signal was calibrated to $[Ca]_i$ values according to a pseudoratio equation. It was assumed that the $K_d$ value for Fluo-3 was 650 nM at 27 °C and that the resting $[Ca]_i$ was 100 nM, before the cells were treated with thapsigargin and ryanodine.

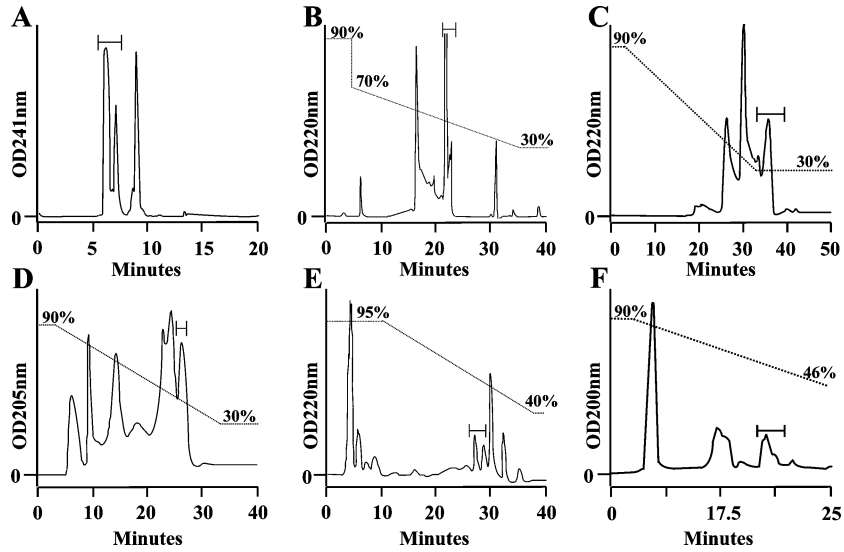


FIGURE 1: HPLC procedures for extensive purification of $NCX_{IF}$. $NCX_{IF}$ was extracted and partially purified by solvent precipitation, gel filtration, and ion exchange procedures, as described in Materials and Methods. Partially purified $NCX_{IF}$ was further loaded on the HPLC columns in the following order: (A) Synergi-Polar (10 mL/min), (B) Krumasil-Silica (5 mL/min), (C) TSK-gel Amide-80 (5 mL/min), (D) ZIC-HILIC (0.5 mL/min), (E) apHera (1.0 mL/min), and (F) Cyclobond (1 mL/min). All other chromatographic conditions are described in Materials and Methods. Aliquots were removed from collected fractions, lyophilized, and then assayed for inhibition of the $Na^+-Ca^{2+}$ exchanger by using the standard assay of $Na_i$-dependent $^{45}Ca$ uptake in sarcolemma vesicles (see Materials and Methods). The active fractions obtained from 20−50 injections were pooled and lyophilized, and then the concentrated fractions were injected into the next column. Bars indicate the fractions containing the inhibitory activity of $NCX_{IF}$.

*Fluo-4 Calibration.* In the confocal microscopy experiments, the average fluorescence per pixel in a scanned line was taken as the observed fluorescence. Before a cardiomyocyte was patched, its autofluorescence was measured under the same scanning conditions as in the following experiment. The $F$ value was taken after subtracting the autofluorescence. Since the emission of Fluo-4 is negligible in the absence of Ca ($F_{min} \sim 0$), the $[Ca^{2+}]_i$ was calculated as $K_d(F)/(F_{max} - F)$. $F_{max}$ was measured directly from each cardiomyocyte at the end of the experiment, as previously outlined (*24, 25*).

*Miscellaneous Assays.* The amount of protein was measured by using a modified method of Lowry (*35*). Fluorescamine was used for detecting the α-amines and peptides (*36*). Reducing sugars were detected with phenol-sulfuric acid reagent (*37*). All analytical assays were downscaled for microplate measurements.

*Statistics.* All data are presented as means ± the standard error of the mean (SEM). Statistical analysis was done by using the Two-Sample *t*-Test (Origin 7.0). *P* values of $<0.05$ were considered to be significant.

## RESULTS

*HPLC Procedures for $NCX_{IF}$ Purification.* The previous purification procedures of $NCX_{IF}$ suffered from inadequate pure separation quality, low loading capacity, and unsatisfactory levels of final yield (*17, 18*). A new set of advanced HILIC columns was introduced to overcome these problems. The new purification scheme is based on combining new preparative (Krumasil-Silica) and analytic (ZIC-HILIC and apHera) HILIC columns with previously explored preparative columns (RP Synergi-Polar and TSK-Amide 80) (Figure 1). The new purification scheme provides a final yield of ~0.03 mg of $NCX_{IF}$/kg of starting material, which is at least 3−4 times higher than the highest yields obtained in previous preparations (*17–23*). A major reason for this improvement is the efficacy of the new HILIC columns, Krumasil-Silica (Figure 1B), ZIC-HILIC (Figure 1D), and apHera (Figure 1E). Despite this progress, currently available quantities of purified $NCX_{IF}$ are still not enough for structural studies by two-dimensional NMR.

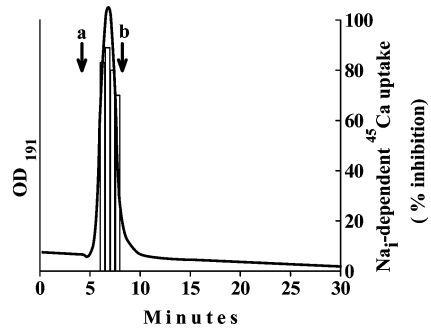


FIGURE 2: Comparison of the HPLC retention time of purified $NCX_{IF}$ with those of the mono- and disaccharide witnesses. The active fractions of $NCX_{IF}$, obtained from the final step of purification (see Figure 1), were loaded on the Aminex HPX-87c column (250 mm × 4 mm, 9$\mu$m) and flashed with water (0.3 mL/min) at 60 °C. Next, the fractions were tested for inhibitory activity of the $Na^+-Ca^{2+}$ exchanger by using the standard assay of $Na^+_i$-dependent $^{45}Ca$ uptake in isolated sarcolemma vesicles (see Materials and Methods). In control samples, the $Na^+-Ca^{2+}$ exchanger activity was assayed under the same experimental conditions with column effluent. Bars indicate the inhibition of $Na^+-Ca^{2+}$ exchanger activity. The straight line indicates continuous detection of effluent from the column at 191 nm. Arrows a and b indicate the retention times of glucose and sucrose, respectively (measured on the same column under identical chromatographic conditions).

The Aminex column is an excellent matrix for separating disaccharide, hexose, and pentose structures. Therefore, an attempt was made to compare the retention time of purified $NCX_{IF}$ to those of known molecular "witnesses" to find any possible correlation between the chromatographic behavior of $NCX_{IF}$ and its chemical structure. The inhibitory activity of $NCX_{IF}$ is eluted as a single peak while showing a complete

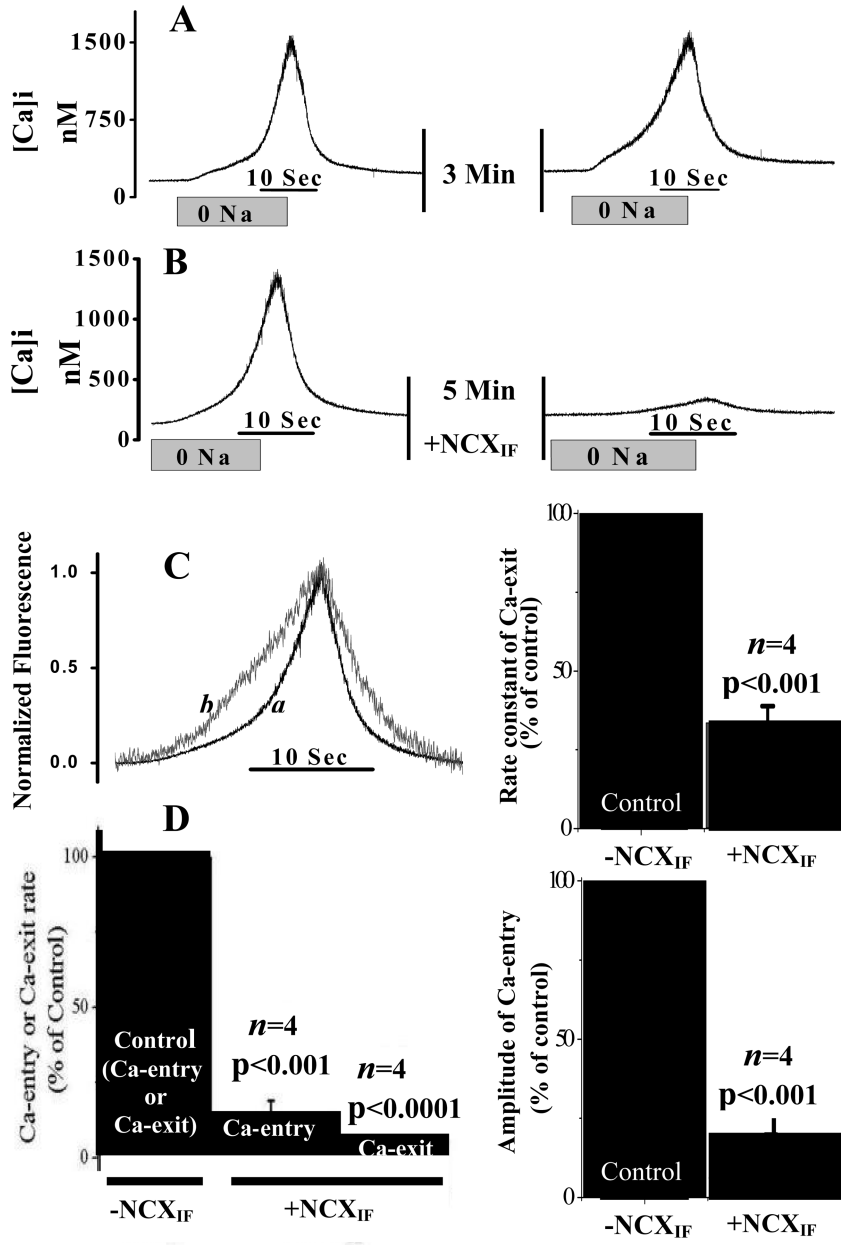


FIGURE 3: $NCX_{IF}$-dependent inhibition of $Ca^{2+}$ entry and $Ca^{2+}$ exit modes of the $Na^+-Ca^{2+}$ exchanger in intact cardiomyocytes. The $Ca^{2+}$ entry and $Ca^{2+}$ exit modes of NCX were monitored in intact cardiomyocytes by perfusing the recording chamber with 0 mM $Na^+$ medium for 20 s (abrupt-0Na). Then the chamber was perfused with normal medium, as indicated, and subsequently, the second session of the $Ca^{2+}$ entry and $Ca^{2+}$ exit reaction was generated in the same cardiomyocyte by switching to the 0 mM $Na^+$ perfusion medium for 20 s. (A) Two consecutive sections of $Na^+$-abrupt reaction in the absence of $NCX_{IF}$. (B) After the first abrupt-0$Na^+$, the recording chamber was perfused with $NCX_{IF}$ (50 units/mL) for 5 min and the $Ca^{2+}$ entry and $Ca^{2+}$ exit reactions were monitored by performing a second abrupt-0Na in the same cardiomyocyte. (C) The data representing the typical effects of $NCX_{IF}$ on $Ca^{2+}$ entry and $Ca^{2+}$ exit modes (see panel B) were normalized. Trace a represents the control before exposure to $NCX_{IF}$, and trace b depicts the recordings obtained after exposure of the same cardiomyocyte to $NCX_{IF}$ (50 units/mL) for 5 min. The $Ca^{2+}$ exit rate constant ($k$) was calculated from the signal obtained by abrupt $Na^+$ removal and is presented as the percentage of the control rate constant. The control rate constant (100%) represents $k = 0.24 \pm 0.047$ $s^{-1}$. (D) Maximal rates (first-derivative) of each reaction are presented as the percentage of control. The control rate (100%) represents $157.1 \pm 37.2$ nM $[Ca^{2+}]_i$ $s^{-1}$ for the $Ca^{2+}$ entry phase and $230.7 \pm 54.8$ nM $[Ca^{2+}]_i$ $s^{-1}$ for the $Ca^{2+}$ exit phase. The amplitude of the $Ca^{2+}$ entry mode was measured in the presence and absence of $NCX_{IF}$ under the conditions described for panel B. The control amplitude (100%) represents the $\Delta[Ca^{2+}]_i$ value of $865.2 \pm 200.9$ nM measured in the absence of $NCX_{IF}$. Results are represented as means $\pm$ SEM. The $n$ values represent the data collected from cardiomyocytes isolated from different animals.

overlap (in time) with optical signals recorded at short UV wavelengths (Figure 2). In general, this kind of overlap of optical signals with inhibitory activity refers to the high quality of the purified substance. Eluted fractions of active $NCX_{IF}$ (Figure 2) exhibit no chemical reactivity with fluorescamine or phenol-sulfur reagent (see Materials and Methods), thereby suggesting no content of the primary amine or aldehyde groups in the purified preparations of $NCX_{IF}$. The chromatographic properties of $NCX_{IF}$ were compared with those of witness molecules (mono-, di-, tri-, and tetrasaccharides) by using the advanced HILIC HPLC columns. The retention time of $NCX_{IF}$ on the ZIC-HILIC (Figure 1D) and Aminex (Figure 2) columns is characteristic of disaccharide-sized molecules. Attempts at structural

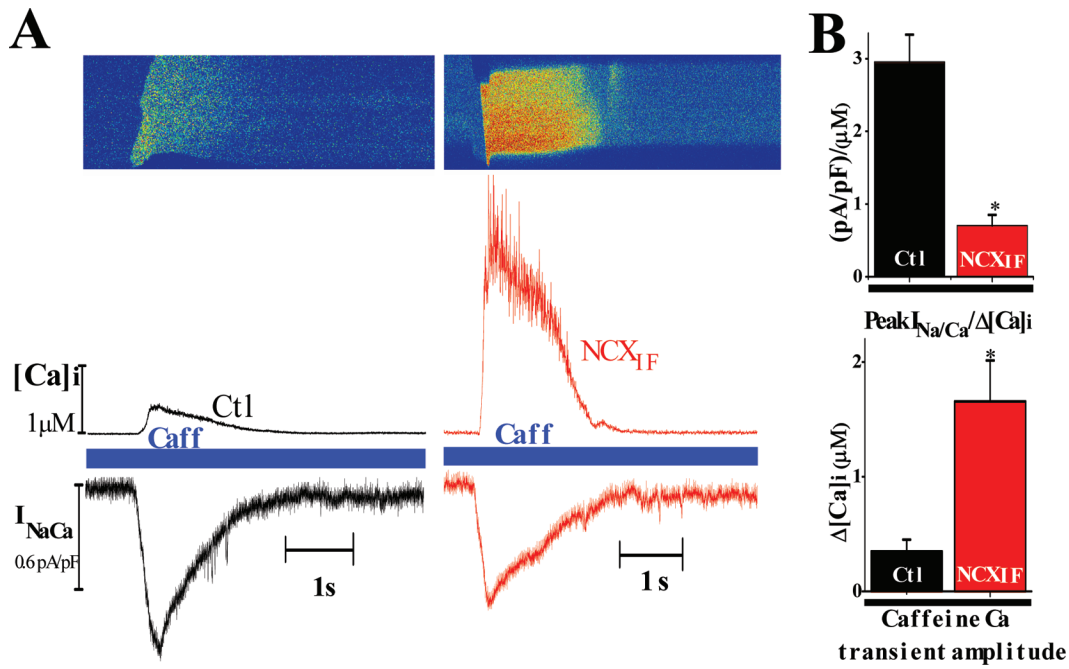


FIGURE 4: Simultaneous recordings of $I_{NCX}$ and $[Ca^{2+}]_i$ in patched cardiomyocytes after transient exposure to caffeine. Adult rat cardiomyocytes were held at −80 mV and loaded with the $Ca^{2+}$ fluorescent dye Fluo-4 through the patch pipet. $Ca^{2+}$ transients were induced by application of 5 mM caffeine (Caff) to a quiescent cell (see Materials and Methods). (A) Typical recordings of $I_{NCX}$ and $[Ca^{2+}]_i$ from a control (left) or $NCX_{IF}$-loaded cell (right). Representative line scan image (top panel), corresponding $[Ca^{2+}]_i$ values (middle trace), and the simultaneously recorded $I_{NCX}$ (bottom trace). (B) The top chart shows the mean peak $I_{NCX}$ normalized to $\Delta[Ca^{2+}]_i$ in control ($n = 10$) and $NCX_{IF}$-loaded cells ($n = 16$; the asterisk indicates a $p$ of $<0.01$). The bottom chart shows the mean values of $Ca^{2+}$ transient amplitudes in control ($n = 10$) and $NCX_{IF}$-loaded cells ($n = 16$; the asterisk indicates a $p$ of $<0.01$). $n$ represents the number of independent experiments.

analysis by LC−MS were not successful due to the extremely weak ionization ability of $NCX_{IF}$.

*Effect of $NCX_{IF}$ on the $Ca^{2+}$ Entry and $Ca^{2+}$ Exit Modes of the $Na^+$−$Ca^{2+}$ Exchanger in Intact Cardiomyocytes.* The $Ca^{2+}$ entry and $Ca^{2+}$ exit modes of NCX1 were monitored in intact cardiomyocytes under conditions in which the SR $Ca^{2+}$ fluxes were completely blocked by pretreatment of cardiomyocytes with ryanodine and thapsigargin (*33, 34*). To assess the $Ca^{2+}$ entry via NCX1, extracellular $Na^+$ was abruptly removed (replaced by TMA) for 20 s and $Ca^{2+}$ entry was monitored by measuring changes in $[Ca^{2+}]_i$ using Fluo-3. Figure 3A shows that $Na^+$ removal results in the elevation of $[Ca^{2+}]_i$ (net $Ca^{2+}$ entry). Following the removal of extracellular $Na^+$, the return of extracellular $[Na]_o$ to normal levels resulted in a decreased $[Ca^{2+}]_i$ and reflects the net exit of $Ca^{2+}$ via the $Na^+$−$Ca^{2+}$ exchanger. Two consecutive series of $Na^+$-abrupt episodes in the same cardiomyocyte (separated by 5 min) produced comparable changes in the amplitude and rates of $[Ca^{2+}]_i$ (Figure 3A). Therefore, the inhibitory effects of $NCX_{IF}$ can be reliably evaluated in the same cardiomyocyte during the second $Na^+$-abrupt episode (the first $Na^+$-abrupt episode can be used as a control). The bidirectional $Ca^{2+}$ fluxes through NCX1 were examined by transient superfusion of cadiomyocytes with extracellular $NCX_{IF}$ (50 units/mL for 5 min). $NCX_{IF}$ significantly reduced the rate and magnitude of the changes in $[Ca^{2+}]_i$ (Figure 3B). $NCX_{IF}$ results in a slowing of the rate of $Ca^{2+}$ entry and of $Ca^{2+}$ exit (Figure 3C). Moreover, $NCX_{IF}$ reduces the amplitude of $[Ca^{2+}]_i$ elevation (to 15.0 ± 4.8% of the control; $p < 0.001$) and decreases the rate of $Ca^{2+}$ entry (11.9 ± 7.2% of the control; $p < 0.001$) and of $Ca^{2+}$ exit (5.6 ± 2.2% of the control; $p < 0.0001$) (Figure 3D). Therefore, $NCX_{IF}$ can effectively inhibit both the $Ca^{2+}$ entry and $Ca^{2+}$ exit modes of NCX1 in intact cardiomyocytes, as expected, on the basis of transport thermodynamics (*50, 51*). These properties of $NCX_{IF}$, which can comparably alter both the $Ca^{2+}$ entry and $Ca^{2+}$ exit modes of NCX1, seem to be very different from the properties of the synthetic NCX blocker, KB-R7943, which exhibits a preferential selectivity for inhibiting the $Ca^{2+}$ entry mode in a single-cardiomyocyte system (*33, 38*).

Although the $Na^+$-abrupt protocol enables us to assess the $Ca^{2+}$ entry and $Ca^{2+}$ exit modes of NCX1 in a single intact cell, this method cannot resolve whether $NCX_{IF}$ interacts with the extracellular or intracellular domain. Therefore, the application of complementary approaches was necessary to resolve the sidedness of $NCX_{IF}$ action in intact cardiomyocytes (see below).

*Direct Loading of $NCX_{IF}$ into the Cytoplasm Inhibits the $I_{NCX}$ and $Ca^{2+}$ Extrusion in Intact Cardiomyocytes.* To further investigate the sidedness of interactions of $NCX_{IF}$ with NCX1, we carried out patch-clamp experiments. Briefly, $NCX_{IF}$ was applied to the interior of intact cardiomyocytes through the patch pipet. In these experiments, $I_{NCX}$ was measured simultaneously with $[Ca^{2+}]_i$ using a combination of patch-clamp and confocal microscopy. Under control conditions, application of caffeine (for 5 s) activates the release of SR $Ca^{2+}$ and elevates $[Ca^{2+}]_i$, consequently enhancing the $Ca^{2+}$-activated inward $I_{NCX}$ current (*24–26*). In patched cardiomyocytes, the cytoplasm was equilibrated with pipet solution containing either no $NCX_{IF}$ (the control group) or 50 units/mL $NCX_{IF}$ (the $NCX_{IF}$ group). Figure 4A shows a typical recording obtained from either a control or a cardiomyocyte loaded with 50 units/mL $NCX_{IF}$. The $[Ca^{2+}]_i$ transient, induced by caffeine, was significantly higher in the $NCX_{IF}$-loaded myocytes [1.66 ± 0.35 $\mu$M ($n = 16$)] than

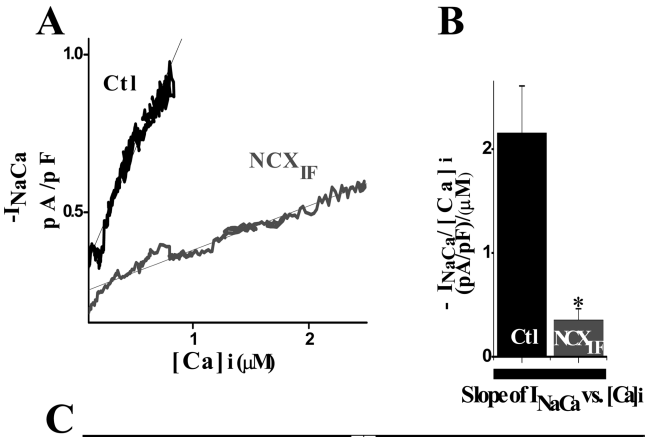


C

| *Control* | | | *$NCX_{IF}$* | | |
|---|---|---|---|---|---|
| [Ca]i range (nM) | Cells No | Exp No | [Ca]i range (nM) | Cells No | Exp No |
| 73-137 | 5 | 8 | 100- 170 | 4 | 11 |
| 141-154 | 5 | 7 | 177- 352 | 4 | 15 |
| 158-186 | 5 | 6 | 366-797 | 3 | 11 |
| 190-229 | 4 | 5 | 799-1165 | 2 | 8 |
| 234-437 | 3 | 4 | 1179-2426 | 1 | 6 |
| 438-762 | 2 | 2 | | | |

FIGURE 5: Effect of directly loading $NCX_{IF}$ into the cytoplasm on $I_{NCX}$ during the $[Ca^{2+}]_i$ increase. Cardiomyocytes were transiently exposed to 5 mM caffeine as described in Materials and Methods. The caffeine-evoked $I_{NCX}$ and $[Ca^{2+}]_i$ values were measured simultaneously and then plotted as indicated. The results represent the rising phase of the caffeine $[Ca^{2+}]_i$ transient (starting from the beginning of $[Ca^{2+}]_i$ upstroke until it peaked). (A) The average values of $I_{NCX}$, obtained at a given $[Ca]_i$ value, were plotted for $NCX_{IF}$-loaded or control ($-NCX_{IF}$) cardiomyocytes as indicated. (B) The slopes of $I_{NCX}$ vs $[Ca^{2+}]_i$ were calculated by fitting the data for each individual experiment ($n = 10$ for control cells and $n = 15$ for $NCX_{IF}$-loaded cells; $p < 0.001$). (C) Different ranges of $[Ca^{2+}]_i$ values (observed in each specific experiment) were plotted vs appropriate levels of $I_{NCX}$, as described for panel A.

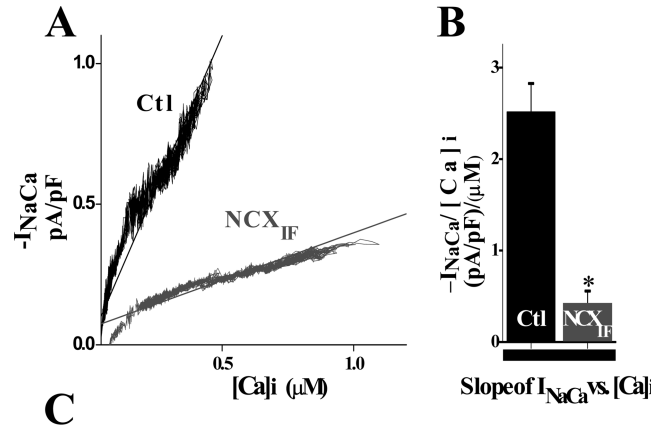


C

| *Control* | | | *$NCX_{IF}$* | | |
|---|---|---|---|---|---|
| [Ca]i range (nM) | Cells No | Exp No | [Ca]i range (nM) | Cells No | Exp No |
| 32-50 | 5 | 7 | 47-181 | 2 | 4 |
| 50-144 | 6 | 8 | 181-497 | 3 | 12 |
| 145-169 | 5 | 7 | 502-815 | 2 | 11 |
| 171-442 | 3 | 4 | | | |
| 443-786 | 2 | 2 | | | |

FIGURE 6: Effect of directly loading $NCX_{IF}$ into the cytoplasm on $I_{NCX}$ during the $[Ca^{2+}]_i$ decline. The caffeine-evoked $I_{NCX}$ and $[Ca^{2+}]_i$ were simultaneously recorded and plotted as described in the legends of Figures 4 and 5. The data were obtained by taking the decline phase of the caffeine-induced $Ca^{2+}$ transient (starting from the $I_{NCX}$ peak until the baseline was reached). (A) The average $I_{NCX}$ values (for given $[Ca^{2+}]_i$ levels) were plotted for $NCX_{IF}$-loaded or control cardiomyocytes ($-NCX_{IF}$). (B) The $I_{NCX}/[Ca^{2+}]_i$ curves were fitted by linear regression, and the obtained slopes were averaged as indicated ($n = 9$ for control cells and $n = 12$ $NCX_{IF}$-loaded cells; $p < 0.001$). The $n$ values represent the number of independent experiments. (C) The observed ranges of $[Ca^{2+}]_i$ values (obtained in each specific experiment) were plotted vs $I_{NCX}$, as described in the legend of Figure 5.

in the control group without $NCX_{IF}$ [$0.34 \pm 0.1$ $\mu$M ($n = 10$; $p < 0.01$)], as shown in Figure 4. The peak $I_{NCX}$ value was insignificantly lower in $NCX_{IF}$-loaded cardiomyocytes ($0.61 \pm 0.05$ pA/pF) than in the control group ($0.79 \pm 0.20$ pA/pF) (data not shown). As shown in Figure 4B, the $I_{NCX}$ per $\Delta[Ca^{2+}]_i$ is much greater in controls than in the presence of $NCX_{IF}$. Therefore, a given concentration of cytosolic $NCX_{IF}$ significantly blocks NCX1 in a single-cardiomyocyte system.

*Effect of $NCX_{IF}$ on the $I_{NCX}-[Ca]_i$ Relationship.* The dependence of $I_{NCX}$ on $[Ca^{2+}]_i$ can be measured dynamically during the time when the application of caffeine increases $[Ca^{2+}]_i$ and its removal leads to a decrease in $[Ca^{2+}]_i$. The data analysis was established by plotting $I_{NCX}$ during the elevation of $[Ca^{2+}]_i$, as shown in Figure 5, and its fall, as shown in Figure 6. Intracellular $NCX_{IF}$ reduces $I_{NCX}$ at any $[Ca^{2+}]_i$ value, consistent with the NCX1 block. The data fitted by linear regression clearly indicate that the slope of $I_{NCX}$ versus $[Ca^{2+}]_i$ is less steep (~6-fold) in $NCX_{IF}$-loaded cardiomyocytes than in control cardiomyocytes in the absence of $NCX_{IF}$. The cytosolic $NCX_{IF}$ has very similar effects on the $I_{NCX}/[Ca^{2+}]_i$ slope during the increase [$6.0 \pm 0.02$-fold change in the slope (Figure 5B)] or the decay phase [$5.94 \pm 0.02$-fold change in the slope (Figure 6B)] of the caffeine-induced $[Ca^{2+}]$ transient. These data clearly indicate that $NCX_{IF}$ inhibits both the NCX-mediated inward current and extrusion of $Ca^{2+}$ from the cell in a comparable way.

At fixed doses of $NCX_{IF}$, the fraction of $I_{NCX}$ inhibition is independent of $[Ca^{2+}]_i$, at least in the tested $[Ca^{2+}]_i$ range of 30−2500 $\mu$M (Figures 5 and 6). This observation provides independent evidence that the degree of inhibition is determined by $NCX_{IF}$ dose and not by $[Ca^{2+}]_i$. As a precaution, one has to take into account that under the experimental conditions tested here, the regulatory sites of NCX1 are fully saturated with cytosolic $Ca^{2+}$. Therefore, a more extensive investigation is required for testing the effects of $NCX_{IF}$ on the interaction of $Ca^{2+}$ with the CBD1 and CBD2 domains.

## DISCUSSION

Purification procedures developed in our laboratory (*17, 18*) permitted primary characterization of $NCX_{IF}$ properties (*17–23*), although these preparations still suffer from weak chromatographic resolution, inadequate pure loading capacity, and low yield. Since milligram quantities of purified $NCX_{IF}$ are required for structural studies, here we describe further improvements in the purification procedures. Although our previous work provided accumulating evidence for the $NCX_{IF}$-induced inhibition of NCX1 activities in vitro (*17–19*) and for the modulation of muscle contractility (*17, 20–23*), there was no evidence for inhibition of NCX1 in the single-cell system. Therefore, this work represents the first attempt at measuring the direct actions of $NCX_{IF}$ on the $Na^+-Ca^{2+}$ exchanger activities in a single-cell system by performing simultaneous measurements of $I_{NCX}$ and cytosolic $[Ca^{2+}]_i$. As predicted from thermodynamic considerations, $NCX_{IF}$ blocks equally well both $Ca^{2+}$ extrusion and $Ca^{2+}$ entry

modes of NCX1 (Figure 3). It appears that $NCX_{IF}$ acts effectively from the cytosolic side (Figures 5 and 6), exhibiting an inhibitory potency that is comparable with the inhibitory potency observed previously with in vitro systems of isolated sarcolemma vesicles (*17–20*). Some issues related to the characteristics of $NCX_{IF}$ action are discussed below.

*Characteristic Properties of Purified $NCX_{IF}$ Preparations.* A several-fold increase in the yield of purified $NCX_{IF}$ preparations was obtained via introduction of new HILIC technologies at various stages of the purification scheme (Figure 1). Despite a significant improvement in preparative procedures, the available amounts of purified $NCX_{IF}$ are still not sufficient for elucidation of the $NCX_{IF}$ structure by two-dimensional NMR. To obtain sufficient (milligram) quantities of $NCX_{IF}$ for structural analysis by NMR, one has to scale up the existing purification procedures at least 5−10-fold (with starting material of 40−50 kg ventricles). Unfortunately, these near-industrial procedures for purification could not be handled in this work due to the lack of available resources.

Another principal problem in molecular identification of $NCX_{IF}$ is that the de novo identification of unknown substances by MS techniques depends on the chemical nature of the investigated substance (*39, 40*). For example, small charged molecules (e.g., such as peptides) can be successfully analyzed even at $10^{-9}$ M, whereas the analysis of hydrophilic, uncharged molecules (e.g., such as small polyols) could be a challenge even at $10^{-3}$ M (*39–41*). If $NCX_{IF}$ is a hydroxyl-rich compound (as we suspect), this would explain why it is so difficult to resolve its structure by MS techniques. Consistent with our previous findings (*18*), $NCX_{IF}$ exhibits very weak absorption only in the short-UV (190−200 nm) range (Figure 2), thereby suggesting that neither aromatic rings (nucleotides, phenols, indols, etc.) nor conjugated chemical groups are present. In agreement with previous analyses (*17, 18*), purified $NCX_{IF}$ (Figure 2) does not react with fluorescamine or phenol-sulfur reagents. Therefore, there is no evidence that $NCX_{IF}$ contains primary amine or aldehyde groups. In potential, the covalent modification of putative hydroxyl groups of $NCX_{IF}$ may enhance the MS and/or NMR signals by 1 order of magnitude, but unfortunately, due to the extremely low solubility of $NCX_{IF}$ in organic solvents (even in pyridine), the chemical modification of hydroxyl group(s) is also not a trivial task.

*$NCX_{IF}$ Inhibits both the $Ca^{2+}$ Entry and $Ca^{2+}$ Exit Modes of NCX1 in Intact Cardiomyocytes.* Although the synthetic NCX blocker KB-R7943 has been reported to preferentially block the $Ca^{2+}$ entry mode of NCX1 in isolated cardiac myocytes (*33, 38*), this explanation is unsatisfactory (*42*), given the requirements of thermodynamics (*50, 51*). This may be explained by the fact that experimental conditions are not sufficiently comparable in the KB-R7943 studies. Here, the conditions for examining both modes of NCX1 action were nearly identical when $NCX_{IF}$ was used to block NCX1. $NCX_{IF}$ blocks equally well for both the $Ca^{2+}$ entry and $Ca^{2+}$ exit modes of NCX1, as shown in Figure 3. Moreover, $NCX_{IF}$ alters not only the rates of $Ca^{2+}$ entry and exit modes but also the rate constants of both modes (Figure 3B). These data suggest that $NCX_{IF}$ may alter the turnover rate constant of the exchange cycle by affecting the rate-limiting step of net ion transport. This is in a good agreement with previous results (*21*), suggesting that $NCX_{IF}$ affects the rate-limiting step of ion translocation without interfering with ion binding at the transport site(s) of NCX1.

*Cytosolic $NCX_{IF}$ Inhibits the NCX1-Mediated Ion Currents at Any Given $[Ca^{2+}]_i$.* $NCX_{IF}$ was directly loaded into the cytoplasm of patched cardiomyoctes to investigate the sidedness of $NCX_{IF}$ action. Inward $I_{NCX}$ was activated by elevation of $[Ca^{2+}]_i$ following transient exposure to caffeine. Simultaneous monitoring of $I_{NCX}$ and $[Ca^{2+}]_i$ has shown that intracellular $NCX_{IF}$ reduces $I_{NCX}$ at any given $[Ca^{2+}]_i$ (Figures 5 and 6). At fixed doses of $NCX_{IF}$, the fraction of $I_{NCX}$ inhibition is independent of $[Ca^{2+}]_i$ (Figures 5 and 6), suggesting that the extent of inhibition is controlled by $NCX_{IF}$ dose and not by cytosolic $Ca^{2+}$ level. The significance of these findings is that $NCX_{IF}$ may interact with some specific cytosolic domain to inhibit NCX1. Notably, the regulatory sites of NCX1 are fully saturated by cytosolic $Ca^{2+}$ under the experimental conditions tested here (Figures 5 and 6). Therefore, the future testing of $NCX_{IF}$ for its capacity to affect the interactions of $Ca^{2+}$ with the CBD1 and CBD2 domains is highly encouraging.

These experiments clearly demonstrate that $NCX_{IF}$ can be effectively "entrapped" inside the cell by direct loading of $NCX_{IF}$ into the cytoplasm of patched cardiomyocyte (Figures 4–6). Although unproven, it seems plausible that an extracellular site of action is unlikely since the extracellular concentration would be significantly reduced by dilution following intracellular administration. In contrast, the extracellular application of $NCX_{IF}$ would tend to load the cell with the inhibitor if it should leak (transport) in, as we suspect it does. This would then explain the efficacy of extracellular application of $NCX_{IF}$ in these experiments describing the bidirectional inhibition of NCX1 (Figure 3). In the absence of $NCX_{IF}$ breakdown, extracellular application of $NCX_{IF}$ should lead to steady-state levels of intracellular $NCX_{IF}$ approaching the extracellular concentration.

*Brief Comparison of $NCX_{IF}$ with Existing NCX Blockers.* A considerable amount of work has been devoted to the development of peptide (*27–32, 42–44*) and organic (*38, 45–47*) NCX blockers; however, all of them have some specific but principal drawbacks. For example, the synthetic blockers (KB-R7943, SEA-0400, and SN-6) inhibit not only NCX but also the other ion transport systems (*38, 48*). Another principal drawback is the enigmatic putative preferential inhibition of the $Ca^{2+}$ entry mode, which would appear to limit its pharmacological significance and utility (*33, 49*). In contrast to the organic NCX blockers, XIP and FRCRCFa can effectively inhibit both the inward and outward currents of NCX by interacting with the cytosolic domain (*42–44*), but these blockers are inactive when added extracellularly due to their impermeability to the cell membrane.

In contrast to the synthetic blocker, KB-R7943, $NCX_{IF}$ results in a comparable inhibition of both the $Ca^{2+}$ entry and $Ca^{2+}$ exit modes in intact cardiomyocytes (Figure 3). Although KB-R7943 and $NCX_{IF}$ are both active when added outside the cell, the striking difference is that KB-R7943 interacts with the extracellular domain, whereas $NCX_{IF}$ might approach the cytosolic site to inhibit NCX1 (Figures 5 and 6). More extensive research is required for comparing $NCX_{IF}$ with the more recently developed NCX inhibitors, SEA0400 and SN-6.

## REFERENCES


1. Carafoli, E. (1987) Intracellular calcium homeostasis. *Annu. Rev. Biochem. 56*, 395–433.
2. Philipson, K. D., and Nicoll, D. A. (2000) Sodium-calcium exchange: A molecular perspective. *Annu. Rev. Physiol. 62*, 111–133.
3. Blaustein, M. P., and Lederer, W. J. (1999) Sodium/calcium exchange: Its physiological implications. *Physiol. Rev. 79*, 763–854.
4. Khananshvili, D. (1998) Structure, mechanism and regulation of the cardiac sarcolemma $Na^+$-$Ca^{2+}$ exchanger, In *Advances in Moleculat and Cell Biology, Life Sciences Program* (Anderson, J. P., Ed.) Vol. 23B, pp 309−356, JAI Press, Inc., New York.
5. Kofuji, P., Lederer, W. J., and Schulze, D. H. (1994) Mutually exclusive and cassette exons underlie alternatively spliced isoforms of the Na/Ca exchanger. *J. Biol. Chem. 269*, 5145–5149.
6. Lee, S. L., Yu, A. S., and Lytton, J. (1994) Tissue-specific expression of $Na^+$-$Ca^{2+}$ exchanger isoforms. *J. Biol. Chem. 269*, 14849–14852.
7. Quednau, B. D., Nicoll, D. A., and Philipson, K. D. (1997) Tissue specificity and alternative splicing of the $Na^+/Ca^{2+}$ exchanger isoforms NCX1, NCX2, and NCX3 in rat. *Am. J. Physiol. 272*, C1250–C1261.
8. Reeves, J. P., and Hale, C. C. (1984) The stoichiometry of the cardiac sodium-calcium exchange system. *J. Biol. Chem. 259*, 7733–7739.
9. Pogwizd, S. M., Schlotthauer, K., Li, L., Yuan, W., and Bers, D. M. (2000) Arrhythmogenesis and contractile dysfunction in heart failure: Roles of sodium-calcium exchange, inward rectifier potassium current and residual $\beta$-adrenergic responsiveness. *Circ. Res. 88*, 1159–1167.
10. Matsuoka, S., Nicoll, D. A., Reilly, R. F., Hilgemann, D. W., and Philipson, K. D. (1993) Initial localization of regulatory regions of the cardiac sarcolemmal $Na^+$-$Ca^{2+}$ exchanger. *Proc. Natl. Acad. Sci. U.S.A. 90*, 3870–3874.
11. Di Polo, R., and Beauge, L. (2002) Ionic ligand interactions with the intracellular loop of the sodium-calcium. Modulation by ATP. *Prog. Biophys. Mol. Biol. 80*, 43–67.
12. Doering, A. E., Eisner, D. A., and Lederer, W. J. (1995) Cardiac Na-Ca exchange and pH. *Ann. N.Y. Acad. Sci. 779*, 182–198.
13. Bers, D. M., and Ginsburg, K. S. (2007) Na:Ca stoichiometry and cytosolic Ca-dependent activation of NCX in intact cardiomyocytes. *Ann. N.Y. Acad. Sci. 1099*, 326–338.
14. Hilge, M., Aelen, J., and Vuister, G. W. (2006) $Ca^{2+}$ regulation in the $Na^+$-$Ca^{2+}$ exchanger involves two markedly different $Ca^{2+}$ sensors. *Mol. Cell 22*, 15–25.
15. Nicoll, D. A., Sawaya, M. R., Kwon, S., Cascio, D., Philipson, K. D., and Abramson, J. (2006) The crystal structure of the primary $Ca^{2+}$ sensor of the $Na^+/Ca^{2+}$ exchanger reveals a novel $Ca^{2+}$ binding motif. *J. Biol. Chem. 281*, 21577–21581.
16. Besserer, G., Ottolia, M., Nicoll, D. A., Chaptal, V., Cascio, D., Philipson, K. D., and Abramson, J. (2007) The second $Ca^{2+}$-binding domain of the $Na^+$-$Ca^{2+}$ exchanger is essential for regulation: Crystal structures and mutational analysis. *Proc. Natl. Acad. Sci. U.S.A. 104*, 18467–18472.
17. Hiller, R., Shpak, C., Shavit, G., Shpak, B., and Khananshvili, D. (2000) An unknown endogenous inhibitor of Na/Ca exchange can enhance the cardiac muscle contractility. *Biochem. Biophys. Res. Commun. 277*, 138–146.
18. Boyman, L., Hiller, R., Shpak, B., Yomtov, E., Shpak, C., and Khananshvili, D. (2005) Advanced procedures for separation and analysis of low molecular weight inhibitor ($NCX_{IF}$) of the cardiac sodium-calcium exchanger. *Biochem. Biophys. Res. Commun. 337*, 936–943.
19. Shpak, C., Hiller, R., Shpak, B., and Khananshvili, D. (2003) The endogenous inhibitor of NCX1 does not resemble the properties of digitalis compound. *Biochem. Biophys. Res. Commun. 308*, 114–119.
20. Shpak, B., Shpak, C., Hiller, R., Boyman, L., and Khananshvili, D. (2004) Inotropic and lusitropic effects induced by the inhibitory factor of the Na/Ca exchanger are not mediated by the $\beta$-adrenergic activation. *J. Cardiovasc. Pharmacol. 44*, 466–472.
21. Shpak, C., Hiller, R., Shpak, B., Boyman, L., and Khananshvili, D. (2004) The low molecular weight inhibitor of NCX1 interacts with a cytosolic domain that differs from the ion-transport site of the Na/Ca exchanger. *Biochem. Biophys. Res. Commun. 324*, 1346–1351.
22. Boyman, L., Hiller, R., Shpak, B., Shpak, C., and Khananshvili, D. (2006) Purified endogenous inhibitor of the Na/Ca exchanger can enhance the cardiomyocytes contractility and calcium transients. *Biochem. Biophys. Res. Commun. 346*, 1100–1107.
23. Shpak, B., Gofman, Y., Shpak, C., Hiller, R., Boyman, L., and Khananshvili, D. (2006) Effects of purified endogenous inhibitor of the $Na^+/Ca^{2+}$ exchanger on ouabain-induced arrhythmias in the atria and ventricle strips of guinea pig. *Eur. J. Pharmacol. 553*, 196–204.
24. Trafford, A. W., Diaz, M. E., and Eisner, D. A. (1999) A novel, rapid and reversible method to measure Ca buffering and time-course of total sarcoplasmic reticulum Ca content ventricular myocytes. *Pluegers Arch. 437*, 501–503.
25. Diaz, M. E., Trafford, A. W., and Eisner, D. A. (2001) The role of intracellular calcium buffers in determining the shape of the cytosolic Ca transient in cardiac ventricular myocytes. *Pluegers Arch. 442*, 96–100.
26. Pogwizd, M., Sipido, K. R., Vendonck, F., and Bers, D. M. (2003) Intracellular Na in animal models of hypertrophy and heart failure: Contractile function and arrhythmogenesis. *Cardiovasc. Res. 57*, 887–896.
27. Khananshvili, D., Shaulov, G., Weil-Maslansky, E., and Baazov, D. (1995) Positively charged cyclic hexapeptides, novel blockers for the cardiac sarcolemma $Na^+$-$Ca^{2+}$ exchange. *J. Biol. Chem. 270*, 16182–16188.
28. Khananshvili, D., Mester, B., Saltoun, M., Shaulov, G., and Baazov, D. (1997) Inhibition of the cardiac sarcolemma $Na^+$-$Ca^{2+}$ exchanger by conformationally constraint small peptides. *Mol. Pharmacol. 51*, 126–131.
29. Khananshvili, D. (1990) Distinction between the two basic mechanisms of cation transport in the cardiac $Na^+$-$Ca^{2+}$ exchange system. *Biochemistry 29*, 2437–2442.
30. Khananshvili, D., Shaulov, G., and Weil-Maslansky, E. (1995) Rate-limiting mechanisms of exchange reactions in the cardiac sarcolemma $Na^+$-$Ca^{2+}$ exchanger. *Biochemistry 34*, 10290–10297.
31. Khananshvili, D., Baazov, D., Weil-Maslansky, E., Shaulov, G., and Mester, B. (1996) Rapid interaction of FRCRCFa with cytosolic side of the cardiac sarcolemma $Na^+$-$Ca^{2+}$exchanger blocks the ion transport without preventing the binding of either sodium or calcium. *Biochemistry 35*, 15933–15940.
32. Khananshvili, D., Price, D. C., Greenberg, M. J., and Sarne, Y. (1993) Phe-Met-Arg-Phe-$NH_2$ (FMRFa)-related peptides inhibit $Na^+$-$Ca^{2+}$ exchange in cardiac sarcolemma vesicles. *J. Biol. Chem. 268*, 200–205.
33. Satoh, H., Ginsburg, K. S., Qing, K., Terada, H., Hayashi, H., and Bers, D. M. (2000) KB-R7943 block of $Ca^{2+}$ influx via $Na^+$-$Ca^{2+}$ exchange does not alter twitches or glycoside inotropy but prevents $Ca^{2+}$overload in rat ventricular myocytes. *Circulation 101*, 1441–1446.
34. Li, S. Z., Wu, F., Wang, B., Wei, G. Z., Jin, Z. X., Zang, Y. M., Zhou, J. J., and Wong, T. M. (2007) Role of reverse mode $Na^+/Ca^{2+}$ exchanger in the cardioprotection of metabolic inhibition preconditioning in rat ventricular myocytes. *Eur. J. Pharmacol. 561*, 14–22.
35. Markwell, M. A., Haas, S. M., Bieber, L. L., and Tolbert, N. E. (1978) A modification of the Lowry procedure to simplify protein determination in membrane and lipoprotein samples. *Anal. Biochem. 87*, 206–210.
36. Udenfriend, S., Stein, S., Bohlen, P., Dairman, W., Leimgruber, W., and Weigele, M. (1972) A reagent for assay of amino acids, peptides, proteins, and primary amines in the picomole range. *Science 178*, 871–872.
37. Fox, J. D., and Robyt, J. F. (1991) Miniaturization of three carbohydrate analyses using a microsample plate reader. *Anal. Biochem. 195*, 93–96.
38. Iwamoto, T., Watano, T., and Shigekawa, M. (1996) A novel isothiourea derivative selectively inhibits the reverse mode of $Na^+/Ca^{2+}$ exchange in cells expressing NCX1. *J. Biol. Chem. 271*, 22391–22397.
39. Hemström, P., and Irgum, K. (2006) Hydrophilic interaction chromatography. *J. Sep. Sci. 29*, 1784–1821.
40. Zwiener, C., and Frimmel, F. (2004) LC-MS analysis in the aquatic environment and in water treatment technology: A critical review. Part II: Applications for emerging contaminants and related pollutants, microorganisms and humic acids. *Anal. Bioanal. Chem. 378*, 851–861.
41. Cech, N. B., and Enke, C. G. (2001) Practical implications of some recent studies in electrospray ionization fundamentals. *Mass Spectrom. Rev. 20*, 362–387.

42. Li, Z., Nicoll, D. A., Collins, A., Hilgemann, D. W., Filoteo, A. G., Penniston, J. T., Tomich, J. M., and Philipson, K. D. (1991) Identification of a peptide inhibitor of the cardiac sarcolemmal $Na^+$-$Ca^{2+}$ exchanger. *J. Biol. Chem. 266*, 1014–1020.

43. Hobai, I. A., Khananshvili, D., and Levi, A. J. (1997) The peptide 'FRCRCFa', dialyzed intracellularly, inhibits the Na/Ca exchange with high affinity in rabbit ventricular myocytes. *Pluegers Arch. 433*, 455–463.

44. Meszaros, J., Khananshvili, D., and Hart, G. (2001) Mechanisms underlying delayed afterdepolarizations in hypertrophied left ventricular myocytes of the rat heart. *Am. J. Physiol. 281*, H903–H914.

45. Watano, T., Kimura, J., Morita, T., and Nakanishi, H. (1996) A novel antagonist, No. 7943, of the $Na^+/Ca^{2+}$ exchange current in guinea-pig cardiac ventricular cells. *Br. J. Pharmacol. 119*, 555–563.

46. Matsuda, T., Arakawa, N., Takuma, K., Kishida, Y., Kawasaki, Y., Sakaue, M., Takahashi, K., Takahashi, T., Suzuki, T., Ota, T., Hamano-Takahashi, A., Onishi, M., Tanaka, Y., Kameo, K., and Baba, A. (2001) SEA0400, a novel and selective inhibitor of the $Na^+$-$Ca^{2+}$ exchanger, attenuates reperfusion injury in the in vitro and in vivo cerebral ischemic models. *J. Pharmacol. Exp. Ther. 298*, 249–256.

47. Iwamoto, T., Inoue, Y., Ito, K., Sakaue, T., Kita, S., and Katsuragi, T. (2004) The exchanger inhibitory peptide region-dependent inhibition of $Na^+/Ca^{2+}$ exchange by SN-6 [2-[4-(4-nitrobenzyloxy)benzyl]thiazolidine-4-carboxylic acid ethyl ester], a novel benzyloxyphenyl derivative. *Mol. Pharmacol. 66*, 45–55.

48. Reuter, H., Henderson, S. A., Han, T., Matsuda, T., Baba, A., Ross, R. S., Goldhaber, J. I., and Philipson, K. D. (2002) Knockout mice for pharmacological screening: Testing the specificity of $Na^+$-$Ca^{2+}$ exchange inhibitors. *Circ. Res. 91*, 90–92.

49. Sipido, K. R., Varro, A., and Eisner, D. (2006) Sodium calcium exchange as a target for antiarrhythmic therapy. *Handb. Exp. Pharmacol.,* 159–199.

50. Noble, D., and Blaustein, M. P. (2007) Directionality in drug action on sodium-calcium exchange. *Ann. N.Y. Acad. Sci. 1099*, 540–543.

51. Ruknudin, A. M., Wei, S. K., Haigney, M. C., Lederer, W. J., and Schulze, D. H. (2007) Phosphorylation and other conundrums of Na/Ca exchanger, NCX1. *Ann. N.Y. Acad. Sci. 1099*, 103–118.

BI8004279